The EMBO Journal (2007) 26, 4038–4050 | © 2007 European Molecular Biology Organization | Some Rights Reserved 0261-4189/07
www.embojournal.org

THE EMBO JOURNAL

EMBO open

The CNS glycoprotein Shadoo has PrP^C-like protective properties and displays reduced levels in prion infections

Joel C Watts[1,2], Bettina Drisaldi[1], Vivian Ng[1], Jing Yang[1], Bob Strome[1], Patrick Horne[1], Man-Sun Sy[3], Larry Yoong[1], Rebecca Young[4], Peter Mastrangelo[1], Catherine Bergeron[1,2], Paul E Fraser[1,5], George A Carlson[4], Howard TJ Mount[1,6], Gerold Schmitt-Ulms[1,2] and David Westaway[1,2,7,*]

[1]Centre for Research in Neurodegenerative Diseases, University of Toronto, Toronto, Canada, [2]Department of Laboratory Medicine and Pathobiology, University of Toronto, Toronto, Canada, [3]Department of Pathology, School of Medicine, Case Western Reserve University, Cleveland, OH, USA, [4]McLaughlin Research Institute, Great Falls, MT, USA, [5]Department of Medical Biophysics, University of Toronto, Toronto, Canada, [6]Department of Medicine, University of Toronto, Toronto, Canada and [7]Centre for Prions and Protein Folding Diseases, University of Alberta, Alberta, Canada

The cellular prion protein, PrP^C, is neuroprotective in a number of settings and in particular prevents cerebellar degeneration mediated by CNS-expressed Doppel or internally deleted PrP ('ΔPrP'). This paradigm has facilitated mapping of activity determinants in PrP^C and implicated a cryptic PrP^C-like protein, 'π'. Shadoo (Sho) is a hypothetical GPI-anchored protein encoded by the *Sprn* gene, exhibiting homology and domain organization similar to the N-terminus of PrP. Here we demonstrate *Sprn* expression and Sho protein in the adult CNS. Sho expression overlaps PrP^C, but is low in cerebellar granular neurons (CGNs) containing PrP^C and high in PrP^C-deficient dendritic processes. In *Prnp*$^{0/0}$ CGNs, Sho transgenes were PrP^C-like in their ability to counteract neurotoxic effects of either Doppel or ΔPrP. Additionally, prion-infected mice exhibit a dramatic reduction in endogenous Sho protein. Sho is a candidate for π, and since it engenders a PrP^C-like neuroprotective activity, compromised neuroprotective activity resulting from reduced levels may exacerbate damage in prion infections. Sho may prove useful in deciphering several unresolved facets of prion biology.

The EMBO Journal (2007) **26,** 4038–4050. doi:10.1038/sj.emboj.7601830; Published online 16 August 2007
Subject Categories: proteins; molecular biology of disease
Keywords: neuroprotection; prions; PrP; scrapie

*Corresponding author. Centre for Prions and Protein Folding Diseases, University of Alberta, Room 116, Environmental Engineering Building, Edmonton, Alberta, Canada T6G 2M8. Tel.: +780 492 9377; Fax: +780 492 9352; E-mail: david.westaway@ualberta.ca

Received: 6 March 2007; accepted: 24 July 2007; published online: 16 August 2007

Introduction

Prions are the causative agents of neurodegenerative diseases, which include bovine spongiform encephalopathy (BSE) in cattle, scrapie in sheep, chronic wasting disease in mule deer and elk, and Creutzfeldt–Jakob Disease (CJD) in humans. The infectious agent is believed to consist of improperly folded forms of a host-encoded protein, the cellular prion protein (PrP^C). Conversion of PrP^C into the disease-associated isoform, PrP^{Sc}, is thought to be the primary pathogenic event, although the mechanisms by which PrP^{Sc} causes disease are poorly understood. PrP^C is absolutely required for disease progression, as PrP knockout (*Prnp*$^{0/0}$) mice do not succumb to disease and do not propagate infectivity following intracerebral challenge with infectious prions (Büeler *et al*, 1992, 1993).

The mammalian prion protein family currently consists of two proteins: PrP^C which is expressed at high levels in the central nervous system (CNS), and Doppel (Dpl), a molecule with a similar three-dimensional structure, whose postnatal expression is normally confined to the testis (Silverman *et al*, 2000; Mo *et al*, 2001). Whereas a role for Dpl in the proper functioning of the male reproductive system has been confirmed in two lines of Dpl knockout mice (Behrens *et al*, 2002; Paisley *et al*, 2004), the function of PrP^C, a well-conserved neuronal glycoprotein, comprises a conundrum, in part because phenotypic alterations in *Prnp*$^{0/0}$ mice have been subtle or disputed. One emerging area of consensus concerns a protective effect of PrP^C against neuronal insults. In particular, PrP^C is upregulated following ischemic brain damage, in both humans and mice (McLennan *et al*, 2004; Weise *et al*, 2004). PrP^C deficiency in mice increases infarct size following cerebral artery occlusion and increases caspase 3 activation (Spudich *et al*, 2005), and PrP^C overexpression improves neurological behavior and reduces infarct volume in a rat stroke model (Shyu *et al*, 2005). Another widely observed and perhaps related phenomenon involves the ability of PrP^C to protect against a variety of proapoptotic stimuli (Kuwahara *et al*, 1999; Bounhar *et al*, 2001; Chiarini *et al*, 2002; Cui *et al*, 2003; Sakudo *et al*, 2005; Lee *et al*, 2006; Novitskaya *et al*, 2006). Strong evidence for a neuroprotective activity for PrP^C against apoptosis *in vivo* has come from studies of transgenic (Tg) mice expressing internally deleted forms of PrP or wild-type (wt)Dpl within the CNS. The presence of Dpl in the brain of *Prnp*$^{0/0}$ mice leads to a neurodegenerative syndrome characterized by a profound apoptotic loss of cerebellar cells (Nishida *et al*, 1999; Moore *et al*, 2001; Rossi *et al*, 2001). A similar phenotype is observed when N-terminally truncated versions of PrP^C (ΔPrP) are expressed in the brain (Shmerling *et al*, 1998). Remarkably, both syndromes are abrogated by the coexpression of wt PrP^C. Recently, it has

been shown that a smaller deletion restricted to the well-conserved central domain of PrP is sufficient to elicit a highly toxic phenotype in *Prnp*$^{0/0}$ mice (Baumann *et al*, 2007; Li *et al*, 2007). The above studies have led to a model in which Dpl and ΔPrP initiate aberrant signaling through a hypothetical prion ligand termed L_{PrP}, a process which is blocked by PrP^C binding (Flechsig *et al*, 2004). Assuming that the interaction between PrP^C and L_{PrP} represents an essential physiological event, the authors also proposed the existence of a PrP^C-like protein termed π, which binds to L_{PrP} and is capable of compensating for the absence of PrP^C in *Prnp*$^{0/0}$ mice. To this date, no candidates for π (or L_{PrP}) have been put forward. However, an open reading frame was discovered which, when translated, exhibits homology to the central hydrophobic domain in PrP^C. This gene, denoted *Sprn* ('shadow of the prion protein'), is present from zebrafish to humans and is predicted to encode a short protein, Shadoo (Sho) (Premzl *et al*, 2003). *Sprn* is located on chromosome 7 in mice, away from the *Prn* gene complex on chromosome 2.

Building on the genetic interaction between PrP^C and Dpl or ΔPrP, we have established an assay for PrP^C activity in primary cultures of cerebellar granule cells (Drisaldi *et al*, 2004, and references therein). Here, cerebellar granule neurons (CGNs) cultured from *Prnp*$^{0/0}$ mice are transfected with plasmids encoding Dpl or PrP alleles of interest and individual apoptotic events scored. This assay recapitulates the phenotypes produced by multiple PrP alleles in Tg mice, including neurotoxicity of both Dpl and ΔPrP, and neuroprotective activity of PrP^C against the toxicity elicited by either Dpl or ΔPrP. In conjunction with biochemical and histological analyses, we have used the CGN assay to explore the properties of Sho. We now demonstrate that Sho is a GPI-anchored neuronal glycoprotein present in the CNS from early postnatal life. Not only is Sho PrP^C-like in its ability to protect against both Dpl and ΔPrP toxicity in the CGN assay, but it is also strikingly reduced in prion infections.

Results

Sho protein expression in N2a cells and brain

Motivated by the absence of obvious phenotypic defects in adult *Prnp*$^{0/0}$ mice, we considered proteins that might overlap functionally with PrP^C. One criterion was evolutionary conservation. In this regard, bioinformatic analyses by Premzl and co-workers have yielded an interesting candidate in the shape of the *Sprn* open reading frame present in genomic DNA of species from mammals to fish (Premzl *et al*, 2003, 2004; Miesbauer *et al*, 2006) and which, unlike the hypothetical *Prnt* gene (Makrinou *et al*, 2002; Premzl *et al*, 2004), is present in the mouse genome. The architecture of the predicted Sho protein loosely resembles the flexibly disordered PrP N-terminus (Figure 1). Analyses of *Sprn* expression by RT–PCR (Premzl *et al*, 2003) and interrogation of expressed sequence tag databases (UniGene) imply expression in embryonic and adult neuronal tissue as well as the retina and visual cortex, but have yet to document spliced mRNAs. Consequently, we evaluated Sho as a putative third member of the prion gene family.

To address expression at the protein level, we raised antibodies against Sho. Two antisera ('04SH-1' and '06SH-3') were

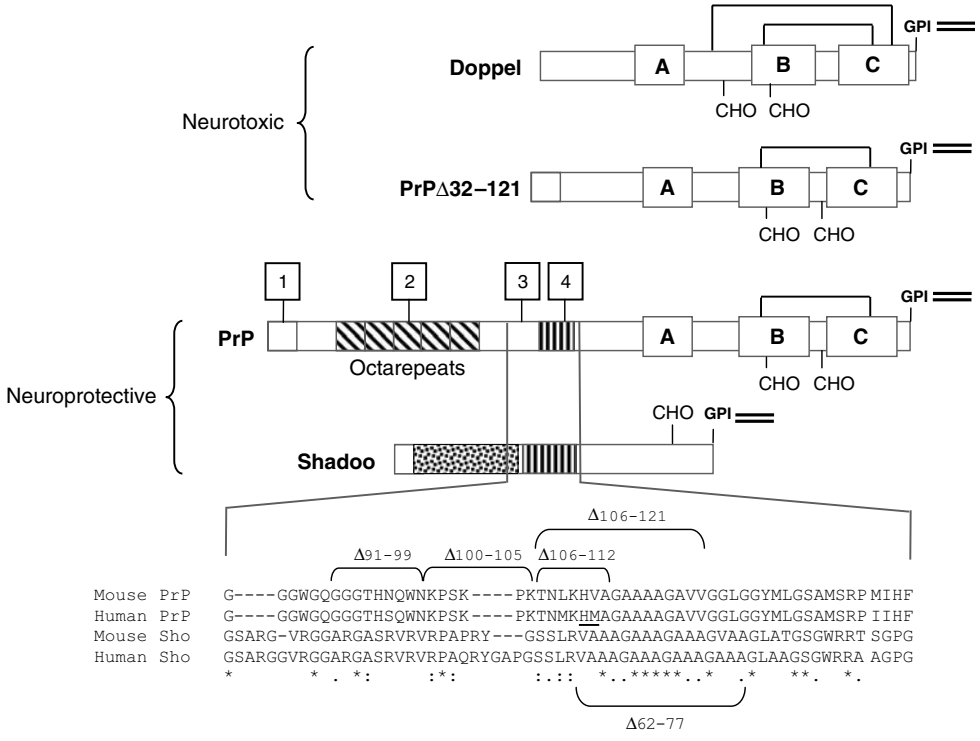

Figure 1 Domain structure of Dpl, PrPΔ32–121, PrP and Sho. α-Helices (A, B and C) are boxed. A basic repeat region in Sho is stippled and the hydrophobic domain in PrP and Sho is striped. Neuroprotective 'determinants', sequences required for PrP's neuroprotective action and mapped genetically, are shown in boxed numbers, and an expanded view shows the central hydrophobic regions of PrP and Sho aligned with the T-COFFEE algorithm. PrP and Sho deletions used in this study are bracketed alongside the alignment. Two residues that correspond to the N-termini of human PrP 'C1' fragment are underlined. 'Neurotoxic' and 'neuroprotective' refer to assays in cerebellar granule cell cultures or Tg mice (see main text).

against a mouse Sho peptide consisting of residues 86–100, whereas a third ('06rSH-1') was against full-length recombinant mouse Sho(25–122) expressed in *Escherichia coli* (Figure 2A) and recognizes an N-terminal epitope contained within residues 30–61 (Supplementary Figure S1). Assessed by Western blot of tissue lysates, 06rSH-1 was virtually devoid of cross-reactive species (Supplementary Figure S1). Cross-reactive species of molecular weights incompatible with authentic Sho were present in analyses with antisera 04SH-1 and with 06SH-3, but these had varying intensities and/or different molecular weights for the two antisera. Consequently, the following comments are restricted to signals detected by two or more varieties of α-Sho antibodies.

Similar to PrP^C, murine Sho is revealed as being expressed at the cell surface, *N*-glycosylated and sensitive to the GPI anchor cleaving enzyme phosphatidylinositol-specific phospholipase C (PI-PLC) in transfected N2a neuroblastoma cells (Figure 2C–E). Following PNGaseF treatment, full-length Sho has a molecular weight of 9.1 kDa as assessed by SDS–PAGE (predicted 9.5 kDa). In addition to the full-length protein, a fraction of the protein in transfected N2a cells has a faster electrophoretic mobility (Figure 2E). In PrP, a well-documented physiological 'C1' cleavage occurs just before the hydrophobic tract at residues His111 and Met112 (human PrP numbering scheme, underlined; Figure 1) both in cultured cells and in the adult brain (Pan *et al*, 1992; Chen *et al*, 1995; Vincent *et al*, 2000). Since cell lysates for these analyses were prepared in the presence of protease inhibitors, it is possible that an analogous endoproteolytic processing could figure in the biogenesis of Sho. A detailed description of truncated forms of Sho will be presented elsewhere (Coomaraswamy *et al*, in preparation).

Analysis of mouse tissue by Western blotting defined a predominant glycosylated protein species of similar molecular weight to transfected full-length Sho (approximately 18 kDa), and one that is developmentally regulated, appearing at embryonic day 16 and persisting in early postnatal life and in the brains of adults (Figure 3A and B). PNGaseF-sensitive bands of identical molecular weights were observed with two independent Sho antibodies, confirming the authenticity of the bands and the presence of Sho in the mouse CNS. Sho signal was emphasized in membrane-enriched preparations from adult mouse brains, corroborating its membrane anchorage (Figure 3C). In Western blots performed with α-Sho86–100 antisera, Sho signal increased following treatment with PNGaseF, suggesting that *N*-glycosylation at Asn107 partially occludes antibody binding at the adjacent epitope for the peptide-directed antiserum.

Overlapping and complementary PrP^C/Sho expression

In situ hybridization using antisense-strand riboprobes prepared against the mouse *Sprn* open reading frame (but not sense-strand controls) yielded signals in the adult mouse CNS. Analyses of the hippocampus and cerebellum revealed prominent signals in the cell bodies of pyramidal cells and

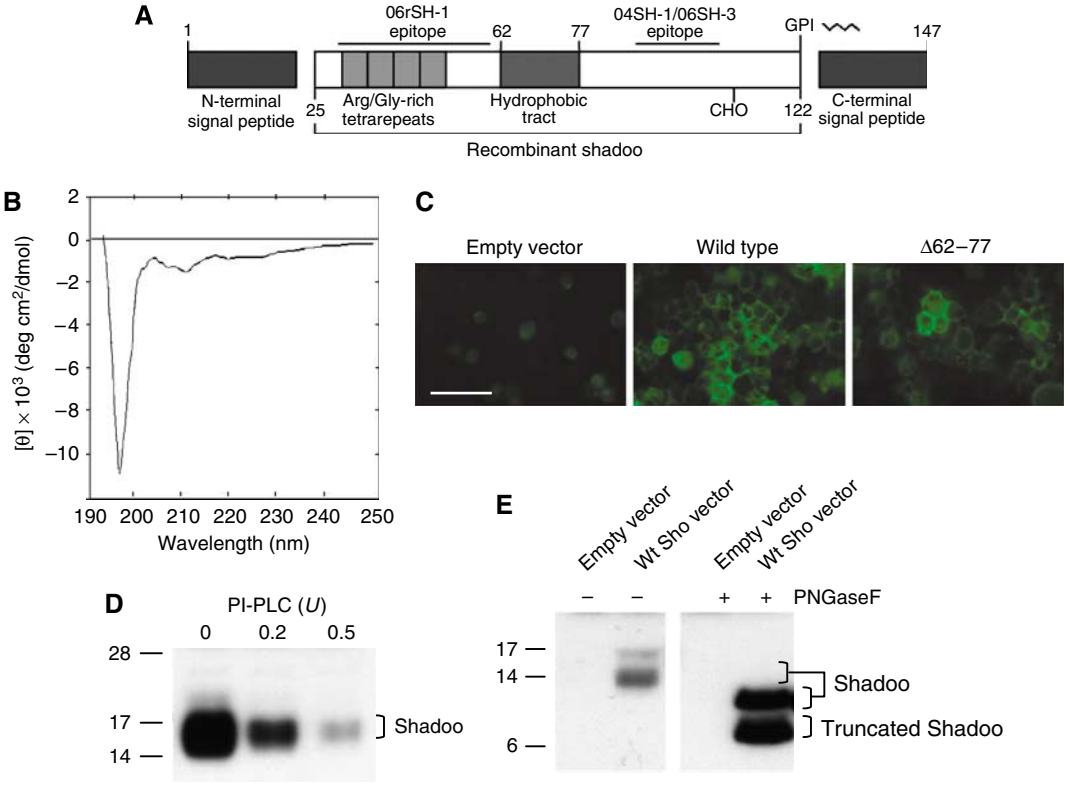

Figure 2 Analysis of recombinant Sho in *E. coli* and expression of murine Sho in cultured cells. (**A**) Schematic representation of the Sho protein. The location of the mapped epitopes for α-Sho peptide antisera (04SH-1 and 06SH-3) and α-recombinant Sho (06rSH-1) are shown. (**B**) Circular dichroism spectrum of recombinant mouse Sho, rSho(25–122). The spectral trace is consistent with a random coil configuration. (**C**) Cell surface expression of wt Sho and a mutant Sho allele lacking the hydrophobic tract in non-permeabilized transfected N2a cells as demonstrated by immunocytochemistry. Scale bar, 50 microns. (**D**) Diminution of Sho signal in the cell lysates of Sho-transfected N2a cells following pretreatment with increasing concentrations of PI-PLC. (**E**) Western blot showing expression of a wt Sho transgene in N2a cells with or without PNGaseF treatment. A lysate from cells transfected with empty vector is included to show antibody specificity.

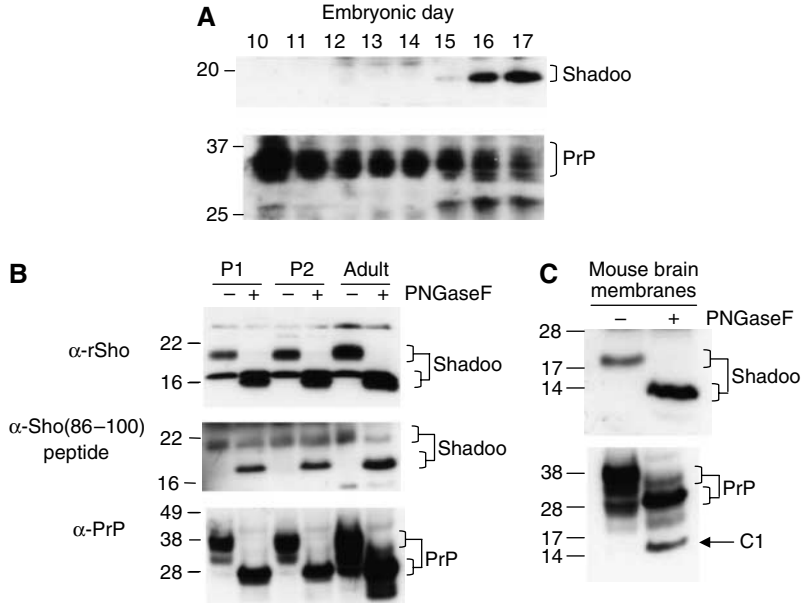

Figure 3 Analysis of mouse Sho in tissue preparations. (**A**) Expression of Sho in whole mouse embryos assessed by Western blotting using a 12% Tris–glycine gel. Sho is expressed beginning at embryonic day 16. (**B**) Postnatal expression of Sho in neonatal and adult mouse brains with or without PNGaseF treatment assessed by Western blotting using 14% Tris–glycine (α-rSho) or 4–12% NuPAGE (α-Sho(86–100) peptide and α-PrP) gels. Full-length species before and after enzymatic treatment are bracketed. (**C**) Sho is present in a membrane-enriched fraction prepared from mouse brains. Membrane preparations with or without PNGaseF treatment were analyzed on 4–12% NuPAGE gels by Western blotting. Sho was detected using either α-Sho peptide polyclonal 04SH-1 (A–C) or α-recombinant Sho polyclonal 06rSH-1 (B), whereas PrP was probed with single-chain antibodies D13 (A–B) or D18 (C).

Purkinje cells, respectively (Figure 4B and J). By way of comparison, *Prnp* has a broader pattern of neuronal expression (Kretzschmar *et al*, 1986; Taraboulos *et al*, 1992). Immunohistochemistry for Sho protein yielded prominent signals in the same cell types defined by *in situ* hybridization (Figure 4D and L), that is, hippocampal neurons and cerebellar Purkinje cells. In the case of antisera 04SH-1, these signals were absent when antibodies were preincubated in a solution containing the Sho86–100 peptide immunogen (Figure 4C and K). Besides defining Sho as the 'second' cellular prion protein present in neurons of the adult CNS, these data define intracellular transport phenomena, as immunohistochemical signals were present in cell processes in addition to the cell bodies detected by antisense riboprobes (i.e., predicted to contain Sho mRNA). In the case of Purkinje cells, immunostaining was present not only in cell bodies but also prominent in their processes, specifically in the dendritic arborizations present within the molecular layer of the cerebellum (Figures 4L and 5F–H, signals detected with all three antisera). A related phenomenon was observed in the hippocampus, notably in CA1 pyramidal neurons. Here, Sho immunoreactivity was absent from axonal projections (with all three α-Sho antibodies), present in cell bodies (seen by all three α-Sho antibodies), and notable in the apical dendritic processes located in the stratum radiatum of the hippocampus (strong signals with 04SH-1 and 06SH-3, and a less intense signal with 06rSH-1) (Figures 4D and 5A–C).

Since PrP has been reported to possess an unusual property for a GPI-linked protein, the ability to undergo basolateral (dendritic) sorting in polarized cells in distinction to the more typical apical (axonal) sorting, parallel analyses were undertaken for PrP^C and Sho. PrP^C was examined at basal levels from the (endogenous) *Prnp* gene, or expressed from a cosmid transgene of the hamster PrP gene including 25 kb of sequences 5′ to the transcriptional start-site (Scott *et al*, 1989; Prusiner *et al*, 1990). In the case of wt mouse PrP, analyses were performed with 7A12 antibody (Li *et al*, 2000) using *Prnp*$^{0/0}$ mice as negative controls (Figure 4E and M), whereas non-Tg wt mice served as negative controls for the use of the hamster PrP transgene-specific 3F4 antibody (Figure 4G and O). Besides the anticipated differences in signal levels between wt and Tg(SHaPrP)7 mice, the PrP^C-directed antibodies yielded similar expression patterns, with widespread staining throughout the brain. PrP^C was underrepresented in the cell bodies of the pyramidal neurons of the hippocampus but abundantly present in the stratum oriens containing the axonal projections, and also in the radiatum, lacunosum moleculare and molecular layers (Figure 4F and H). In the cerebellum, mouse PrP^C was absent in wt Purkinje cells (as described previously (Liu *et al*, 2001; Baumann *et al*, 2007)) and hamster PrP^C was represented in some but not all Purkinje cells of Tg(SHaPrP)7 mice, and at a level lower than that of the surrounding neuropil (Figure 4N and P). On the other hand, PrP^C was present in the granule cell layer and abundant in the molecular layer. Strikingly, the abundant signal present in the radiatum layer was not totally uniform, and—by virtue of a negative staining effect—revealed the outlines of Purkinje cell dendritic arborizations in the cerebellum and the apical dendritic of CA1 neurons (Figure 5D–E, and I–J): these are structures with marked immunostaining with α-Sho86–100 (04SH-1 and 06SH-3) and α-rSho (06-rSH1); Figure 5A–C and F–H). These data therefore define a complementary 'interlocking' aspect to PrP^C/Sho protein expression in the cerebellum and suggest a similar effect in the hippocampus.

Although the most prominent Sho signals were obtained in the hippocampus and cerebellum (Figure 4), signals for both

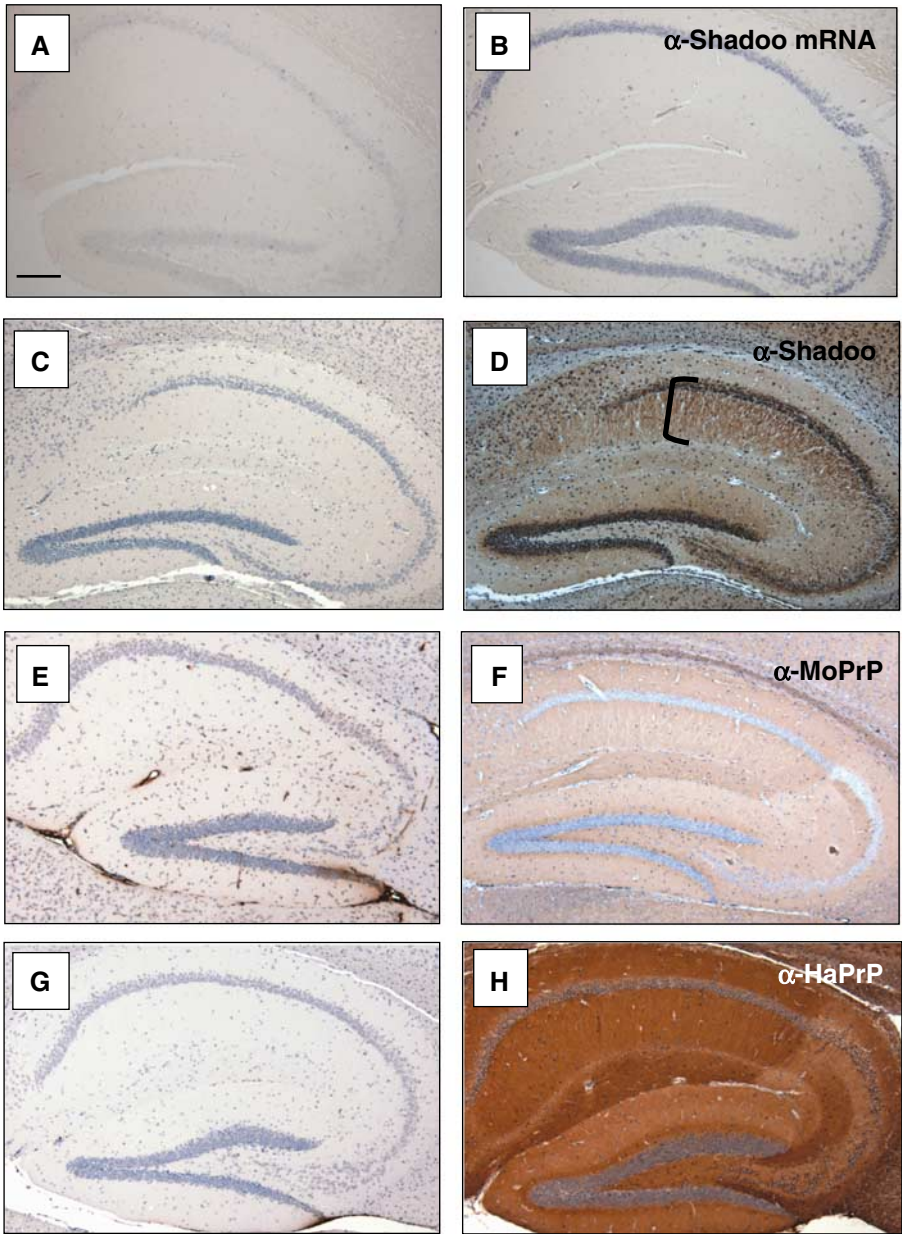

Figure 4 Localization of *Sprn* mRNA and Sho protein in the adult mouse brain. (**A–H**) The hippocampus, and (**I–P**) the cerebellum. wt C57/B6 mice are presented in all sections, with the exception of B6 congenic *Prnp*$^{0/0}$ (E, M) and Tg(SHaPrP)7 mice (H, P). Panels A, C, E, G, I, K, M and O in the left-hand columns comprise negative controls (i.e., sense-strand riboprobes, peptide-directed antisera preincubated with a soluble form of the antigenic peptide, *Prnp*$^{0/0}$ mice for PrP-directed antibodies) for analyses presented in the right-hand columns. *In situ* hybridization: panels A, B, and I, J represent hybridizations with Sho sense-strand (A, I) or antisense (B, J) cRNA probe. Sections are not counterstained and blue staining from NBT/BCIP substrate represents hybridization to *Sprn* mRNA. Immunohistochemistry*:* all other panels of mouse brains with genotypes as noted above. Anti-Sho antibody 04SH-1 (α-Sho) antibody was used with (C, K) or without (D, L) preincubation with Sho(86–100) peptide. Antibodies 7A12 and 3F4 were used for the detection of mouse PrP (E, F, M, N) and hamster PrP (G, H, O, P), respectively. Note the Sho staining of CA1 apical dendritic processes (D, black bracket) and Purkinje cell layer (L, white arrow), and absence of Purkinje cell-body staining with α-moPrP (N) and relative paucity of staining with α-HaPrP antibody (P, black arrow). Scale bar in panels A–H, and I–P, 100 μm.

Sprn mRNA and Sho protein were also present in other areas of the brain including the cerebral cortex, the thalamus, and the medulla (Figure 5L–N; Supplementary Figure S2). Coincidence with neurofilament staining indicates that neurons are the prominent site of Sho expression (Supplementary Figure S2). PrP^C signal was abundant in these regions (Figure 5, and data not shown), confirming that Sho and PrP^C expression profiles overlap in certain areas of the brain. A further example of this phenomenon is apparent in the adult retina (Premzl *et al*, 2003; Chishti *et al*, in preparation). In overview, Sho expression within the adult mouse brain is either less widespread than PrP^C, or basal Sho levels in certain areas fall below the detection threshold of our current procedures. Lastly, to assess whether there is a physiological cross-regulation effect between PrP^C and Sho, we performed a number of analyses on *Prnp*$^{0/0}$ mice (Supplementary Figure S4). These failed to reveal a clear upregulation of Sho in response to PrP^C deficiency.

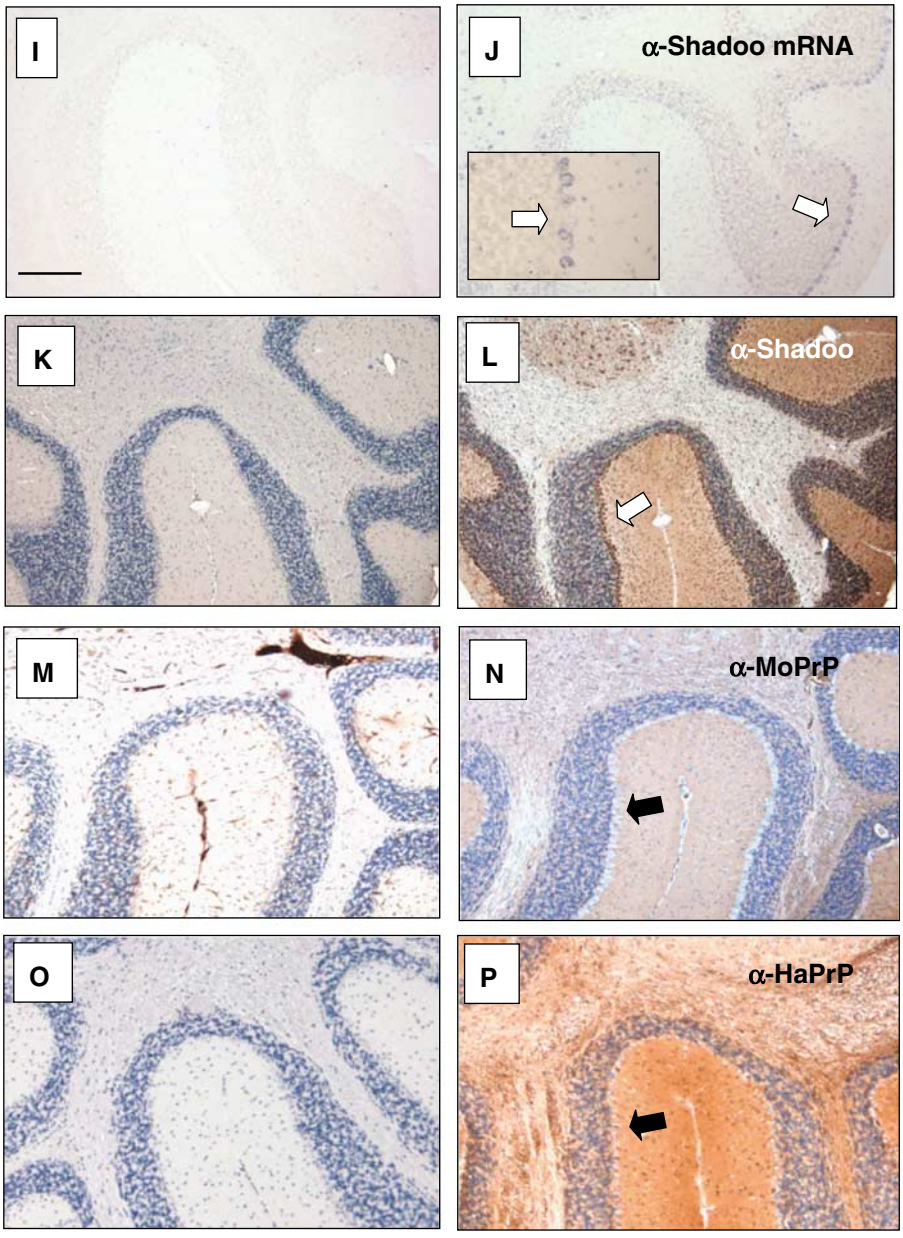

Figure 4 Continued.

Neuroprotective activity and the central region of PrP

Two N-terminal PrP modules, the charged region and the copper-binding octarepeats, contribute to neuroprotective activity in a neuronal assay (Drisaldi *et al*, 2004). However, while others analyzed the same N-terminal modules, they highlighted a trafficking effect (Sunyach *et al*, 2003), so we sought determinants beyond these potential delivery signals. The C-terminus of PrP^C comprises a three-helix bundle (Riek *et al*, 1996) similar to Dpl (Mo *et al*, 2001), and in the form of alleles such as PrPΔ32–121 (Shmerling *et al*, 1998), exhibits Dpl-like toxicity. We therefore focused on the 'remaining' area of PrP, residues 91–121 between the octarepeats and the structured domain (Figure 1) containing the hydrophobic domain (HD) with Sho homology. The deletion alleles were tested for their ability to engender stable forms of PrP. As anticipated from prior analyses of in-frame deletions (Holscher *et al*, 1998; Shmerling *et al*, 1998; Hegde *et al*, 1999), these forms of PrP were synthesized at levels similar to wt PrP, and also underwent similar maturation (Baumann *et al*, 2007; Li *et al*, 2007) (Supplementary Figure S3).

Residues 100–105 are poorly conserved (Figure 1) and in the cerebellar granule neuron (CGN) cellular assay (Drisaldi *et al*, 2004), a PrPΔ100–105 allele exhibited protective activity like wt PrP ($P<0.001$) when measured against Dpl. Conversely, PrPΔ91–99 and PrPΔ106–112 alleles had decreased protective activity (neither is significantly different from Dpl alone; Figure 6B). PrPΔ106–121 transfected alone exhibited partial neurotoxic activity approaching that of a toxic PrPΔ32–121 control allele (Shmerling *et al*, 1998), but different from that of wt PrP ($P<0.01$) (Figure 6A). These data offer a parallel to assays in Tg mice. Here, deletions invading the PrP central region from residues 91 to 121 produce proteins that are progressively toxic: no significant pathological abnormalities are noted in Tg mice expressing PrP Δ32–80, Δ32–93, and Δ32–106, but mice expressing Δ32–121 (or Δ32–134) exhibit profound loss of cerebellar cells

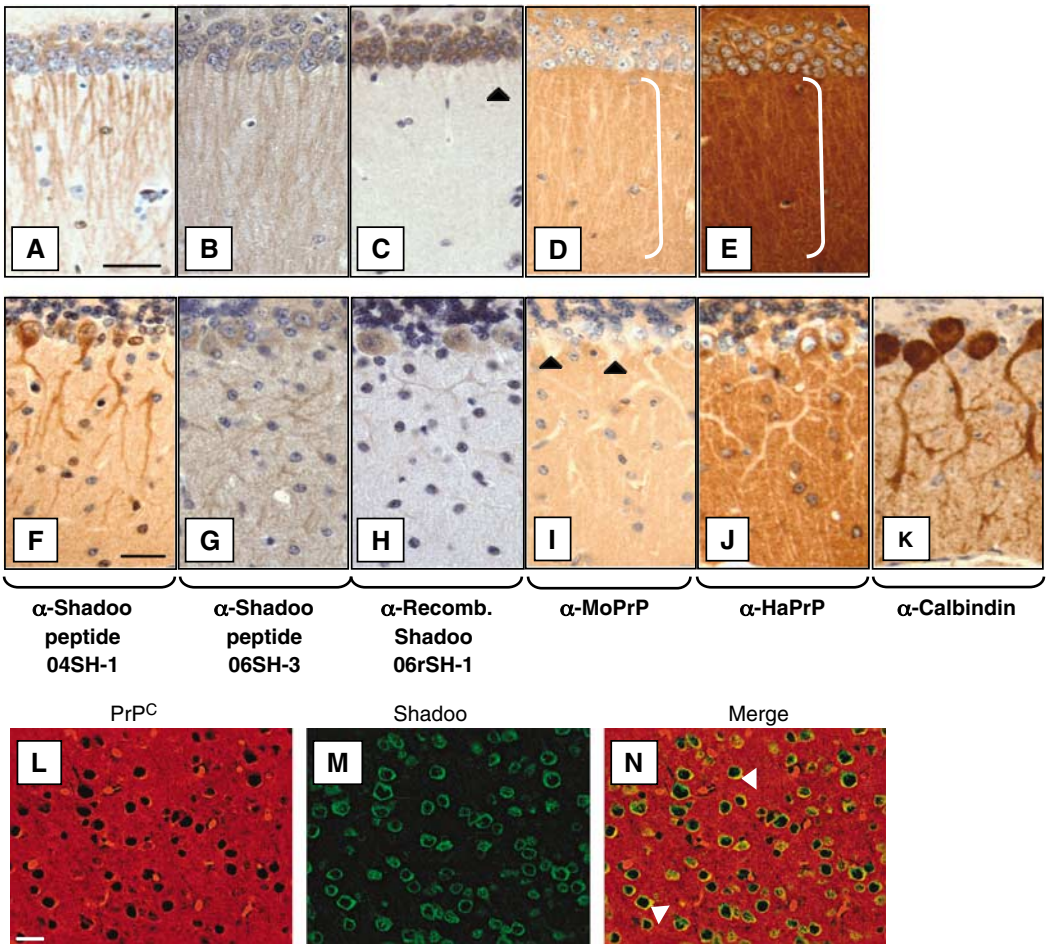

Figure 5 Reciprocal and overlapping expression of Sho and PrP^C in the CNS. (**A–E**) CA1 hippocampal neurons of adult mice probed as indicated. The signal for Sho immunohistochemistry in apical dendrites of wt mice (A–C) has an equivalent in a 'negative image' (white brackets) in the molecular layer of the neuropil imaged for either mouse PrP (D) or hamster PrP in Tg(SHaPrP)7 mice (E). Apical dendrites were less intensely stained with the α-Sho 06rSH-1 antibody (C, black arrowhead) Analogous analyses are presented for Purkinje cells (**F–J**). Somatodendritic localization of Sho in Purkinje cell bodies and dendritic arborizations (F–H) is contrasted by a reciprocal 'negative image' in molecular layer of the neuropil imaged for either mouse PrP (I) or hamster PrP in Tg(SHaPrP)7 mice (J). Note the complete absence of MoPrP staining in cell bodies (I, black arrowheads). Somatodendritic localization of calbindin in Purkinje cells of wt mice (**K**) is shown for comparative purposes. (**L–N**) The cerebral cortex probed simultaneously with α-Sho (06rSH-1, green) and α-PrP (8H4, red) antibodies. Overlapping PrP^C and Sho expression is observed in neurons of the cerebral cortex, including colocalization in cell bodies (N, white arrowheads). Scale bar, 25 μm (A–E), 10 μm (F–K) or 20 μm (L–N).

(Shmerling *et al*, 1998; Flechsig *et al*, 2004), as do mice expressing PrPΔ94–134 or Δ105–125 (Baumann *et al*, 2007; Li *et al*, 2007). From this we infer that a third determinant of neuroprotection lies between PrP residues 91 and 99, and a complex or modular activity determinant ('determinant 4') lies between residues 106–121, whereby a Δ106–112 deletion loses protective activity and a larger Δ106–121 deletion exhibits partial neurotoxic activity. These data extend observations made in hippocampal neurons, where PrP residues 95–124 were implicated in neuroprotective action versus Dpl (Lee *et al*, 2006).

Sho has PrP^C-like neuroprotective activity in a functional assay

Sequence identity between Sho and PrP occurs in the central hydrophobic region. Since this area is highly conserved in PrP (Wopfner *et al*, 1999) and is predicted to overlap or be immediately adjacent to determinants of neuroprotective action (Figures 1 and 6B), we tested Sho in a functional assay in *Prnp*$^{0/0}$ CGN cultures. Remarkably, a wt mouse Sho cDNA was PrP^C-like in its ability to block the proapoptotic action of cotransfected Dpl (Figure 6B) ($P<0.001$ versus Dpl alone, no significant difference between wt PrP alone versus Dpl + Sho). Since the putative PrP^C-like activity called π was inferred from the action of ΔPrP, rather than the action of Dpl (Shmerling *et al*, 1998), further experiments were carried out to assess the effect of Sho upon the toxic action of a ΔPrP allele (Figure 6C). In these cotransfections, wt Sho reduced the toxic activity of singly transfected PrPΔ32–121 to a baseline defined by 'empty vector' (pBUD.GFP) controls ($P<0.001$), and overlapping expression and colocalization was apparent in transfected neurons (Figure 6E). Besides adding to the similarities between Sho and π, these data underscore the notion that ΔPrP and Dpl exert toxicity through the same pathway.

Given the similarity between Sho and PrP in the HD, this domain was a strong candidate for the 'active site' of Sho. Consequently, we assessed the protective activity of Sho

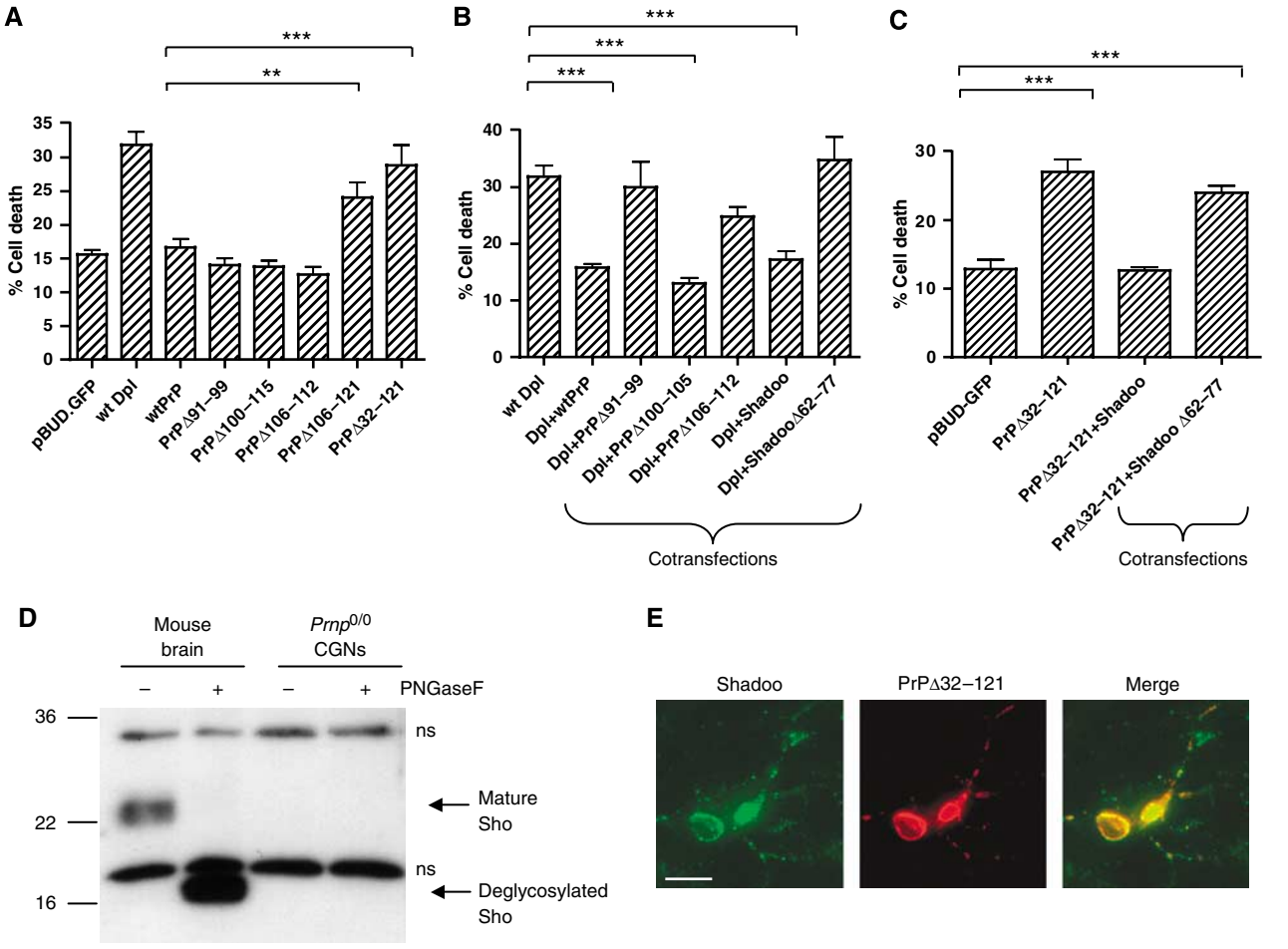

Figure 6 Neuroprotective activity and Sho expression in CGN cells. Test for toxicity of PrP mutant alleles versus the performance of neurotoxic wtDpl and PrPΔ32–121 controls in single transfections (**A**), results of cotransfections of PrP deletion mutants, wt Sho and pBUD.GFP empty vector controls with wtDpl plasmid (**B**), and results of cotransfections to assess putative protective effects of Sho and internally deleted Sho versus a toxic PrPΔ32–121 allele (**C**). Determinations (% cells ± s.e.m undergoing apoptosis) reflect the results of two or more triplicate transfections of independent batches of *Prnp*$^{0/0}$ CGNs scored by independent observers. Whereas PrPΔ100–105 and wt Sho had potent neuroprotective activity (both $P<0.001$, $n=6$, $n=11$, respectively) not significantly different from that of wt PrP, PrPΔ91–99 and PrPΔ106–112 exhibited a tendency for reduced neuroprotective activity against Dpl (neither cotransfection is significantly different than Dpl single transfections). ShoΔ62–77 cotransfections were not significantly different from Dpl or PrPΔ32–121 single transfections. PrPΔ106–121 ($n=11$) transfected alone was significantly different from wt PrP ($P<0.01$; $n=15$) and all other PrP alleles ($P<0.001$), with the exception of the previously documented toxic PrPΔ32–121 allele (Shmerling *et al*, 1998): PrPΔ32–121 ($n=7$) versus wt PrP, $P<0.001$. Cerebellar granule cell assays for bioactivity, creation of plasmid constructs and verification of protein expression were performed as described previously (Drisaldi *et al*, 2004; Supplementary Figure 3) $^{**}P<0.01$, $^{***}P<0.001$. (**D**) Western blot analysis using 06rSH-1 detects Sho in mouse brain lysates but not in a normalized loading of lysate derived from mouse CGNs. 'ns' = non-specific bands detected by the antibody. (**E**) Immunocytochemistry on non-permeabilized CGNs cotransfected with non-fluorescent Sho and PrPΔ32–121 plasmids (3:1 ratio). Sho was detected with 06rSH-1 and PrPΔ32–121 with 8H4. Both Sho and PrPΔ32–121 are expressed in a single cell and colocalization is observed in the cell body. Scale bar, 15 μm.

bearing a precise HD deletion. Here, the cotransfected ShoΔ62–77 allele was not protective against Dpl (not significant versus Dpl alone) (Figure 6B). wt and Δ62–77 Sho alleles are expressed at similar levels in bulk-transfected cells, and with immunoreactivity present upon the surface of transfected N2a cells (Figure 2C; Supplementary Figure S1). In contrast to a wt control allele, the ShoΔ62–77 allele also did not exert significant protection against a toxic PrPΔ32–121 allele ($P<0.001$ versus baseline of pBUD.GFP empty vector; Figure 6C).

As an extrapolation from results presented above and from prior analyses (Nishida *et al*, 1999; Moore *et al*, 2001; Rossi *et al*, 2001), the ability of Dpl to cause cell death in *Prnp*$^{0/0}$ CGNs implies lack of a compensatory neuroprotective activity (e.g., Sho) in these cells. To test this inference, and as an additional control for immunohistochemical analyses presented in Figures 4 and 5, we assessed Sho expression in the lysates of purified CGNs. Although Sho was readily detected in brain lysate, the analysis failed to detect a comparable signal in a normalized loading of CGN lysate (Figure 6D).

Sho expression in prion-infected brains

To assess Sho in a disease setting, Western blots were performed on brain homogenates from wt mice infected with the RML isolate of mouse-adapted prions (Carlson *et al*, 1986). Two independent cohorts produced in different laboratories were used for this analysis. Assessed in the clinical phase of disease, animals from both cohorts demonstrated a striking reduction in Sho protein levels (Figure 7A

and E). Notably, this decrease in signal is apparent using two distinct Sho antibodies with independent epitopes. Normalized against Thy-1, another GPI-anchored neuronal protein, Sho signals of RML-inoculated brain extracts versus brain extracts from healthy controls were reduced eight-fold (Figure 7B). A variety of other neuronal proteins were probed as internal controls (Figure 7C). Although mild loss of signal was apparent for some of these—perhaps a direct consequence of neuronal damage and death—in no instance did these reductions approach those seen for Sho. As a further control we assessed Sho levels in a widely used animal model of Alzheimer's Disease, TgCRND8 mice expressing a mutant β-amyloid precursor protein transgene (Chishti *et al*, 2001). Using mice in clinical phase of the disease (marked by overt amyloid deposits, normalized Aβ levels equaling those of sporadic Alzheimer's disease, and profound cognitive impairment), no difference was apparent between TgCRND8 and non-Tg mice with regards to Sho levels (Figure 7D). Thus, depletion of Sho is absent in non-infectious CNS amyloidosis.

Discussion

Our first conclusion is that Sho is a bona fide neuronal glycoprotein and the third member of the mammalian prion protein family. Beyond mere sequence homology, Sho demonstrates a number of biochemical and cell biological properties also exhibited by PrP^C. These include addition of a GPI anchor, *N*-glycosylation at one or two sites and a cleavage event likely positioned N-terminal to the hydrophobic tract (Figures 1 and 2C–E; Supplementary Figure S1). Furthermore, there are functional redundancies between PrP^C and Sho measured in CGN cells. Although Sho and PrP^C have dissimilar N-terminal regions that may tailor their activities in different neuroanatomic sites, we infer that the center of both PrP^C and Sho comprises a functionally conserved and ancient activity domain contributing to neuroprotection. In PrP^C-deficient areas of the brain, Sho may be particularly important in filling-in a PrP-like activity. Although the exact relevance of PrP^C/Sho neuroprotection against exogenous stimuli versus *in vivo* brain physiology remains to be deciphered, a role against neuronal insults such as ischemic damage seems plausible. Indeed, increased PrP^C expression following stroke has been observed in both humans and mice (McLennan *et al*, 2004; Weise *et al*, 2004).

A second conclusion is that the study of Sho may help decipher the molecular mechanisms underlying physiological signaling from the prion protein family. Here, some initial hints can be inferred from mutational analysis. As deletions invade the central region of PrP^C, not only is protective activity lost, but the mutant PrPs gain spontaneous proapoptotic activity, as shown by loss of the granule cell layer in Tg mice (Flechsig *et al*, 2004), and echoed here by the divergent performance of PrPΔ106–112 and Δ106–121 alleles in the CGN assay. It is possible that a gain of proapoptotic function for PrP within CA1 neurons when it is sterically blocked and dimerized by antibodies against residues 95–105 proceeds by a related mechanism (Solforosi *et al*, 2004). In any event, the PrP^C central region defined by genetic mapping (analyzed by

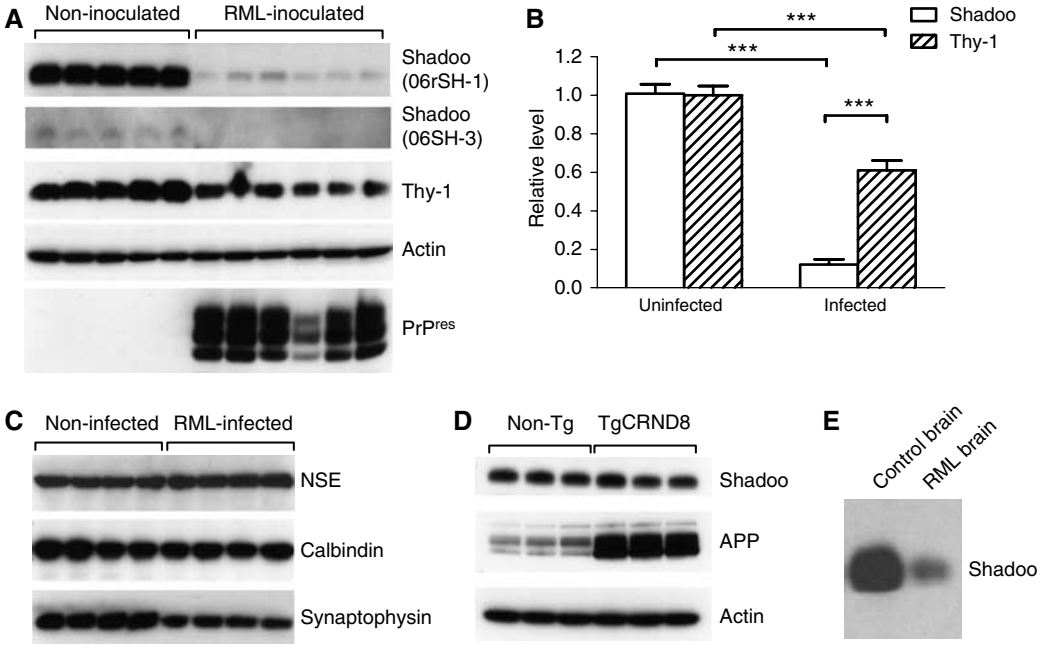

Figure 7 Reduced Sho levels in clinically ill prion-infected mice. (**A**) Western blot of homogenates prepared from the brains of non-inoculated or clinically ill (average of 172 days post-inoculation) RML prion-inoculated mice (C3H/C57BL6 background). Sho protein levels are notably reduced in prion-infected brains. Levels of the GPI-anchored protein Thy-1 are shown for comparison purposes. (**B**) Quantitation of Sho (06rSH-1) and Thy-1 blot signals in panel A by densitometry. Sho levels in prion-infected brains (normalized against Thy-1 signal) are reduced to 12.1±2.8% ($P<0.001$) the levels observed in non-inoculated mice. ***$P<0.001$. (**C**) Expression of neuronal markers in prion-infected and control mouse brains as assessed by Western blotting. No change in neuron-specific enolase (NSE) or calbindin levels, and only a moderate decrease in synaptophysin levels are observed in prion-infected brains. (**D**) No change in Sho levels are observed in brain homogenates prepared from clinically ill (8 months old) Tg mice (TgCRND8) expressing a familial Alzheimer's disease-associated variant of the amyloid precursor protein and control non-Tg littermates. (**E**) Reduced Sho expression in normalized brain homogenates in a second cohort of RML-inoculated mice versus control mice injected with a brain homogenate from healthy mice (C57BL6 background, 154 days post inoculation).

CGN assays in this paper, see also Lee *et al*, 2006) is natively unstructured in NMR studies (Donne *et al*, 1997; Riek *et al*, 1997) and the homologous region in Sho is likely to be natively unstructured as well (Figure 2B). This region may serve as a site for protein–protein interactions, and in this regard, our results parallel and extend a model for signaling from PrP^C protein complexes. Besides PrP^C, this model involves a hypothetical ligand, L_{PrP}, and a conjectural PrP^C-like protein denoted 'π' (Shmerling *et al*, 1998; Flechsig *et al*, 2004). Two docking sites are posited between L_{PrP} and PrP^C, and one docking site between Dpl or ΔPrP and L_{PrP}. Based on sequence similarity and domain structure (Figure 1), biochemical properties (Figure 2), a low level expression of Sho in the cerebellar granule cells (Figures 4L and 6D), and similar effects of wt PrP or Sho versus Dpl or PrPΔ32–121 in CGN assays (Drisaldi *et al*, 2004) (Figure 6B), Sho can be seen to resemble π. In this scheme, sequences within or around the hydrophobic domain of Sho or PrP^C would comprise a docking site for L_{PrP}, a site associated with a protective effect. In PrP^C, partial loss of this site may confer spontaneous neurotoxic behavior, consistent with the enhanced toxicity observed in Tg mice expressing PrP with HD deletions (Baumann *et al*, 2007; Li *et al*, 2007). A second site lying within the α-helical domain present in PrP, ΔPrP and Dpl is associated with a toxic effect (i.e., as per ΔPrP and Dpl) unless the first site is also present (as in wt PrP^C) (Shmerling *et al*, 1998; Cui *et al*, 2003; Drisaldi *et al*, 2004). Even though the original L_{PrP}–PrP^C–π model may prove incorrect in a cell biological sense (i.e., that signaling may have more to do with protection from toxic stimuli rather than regulation of endogenous trophic signals), it provides a useful framework for deciphering molecular interactions. Certainly the ability to now perform studies with PrP, ΔPrP, Dpl and Sho and assess responses within a cellular assay should aid the identification of authentic PrP interactors.

A third conclusion is that Sho may open a window to pathological signaling events in prion disease. Studies of scrapie-infected rodents support the concept of neuroanatomic 'target areas' that give rise to the clinical features of disease (Kimberlin and Walker, 1986). Thus far, the mechanisms by which disease associated forms of PrP (PrP^{Sc} or 'PrP^D') might cause dysfunction in these target areas have proven elusive (Flechsig *et al*, 2000). For example, whereas a requirement for PrP^C was inferred from grafting tissue from mice overexpressing PrP^C into *Prnp*$^{0/0}$ mouse brains and performing prion challenge of chimeric mice (Brandner *et al*, 1996), a genetic reconstitution experiment employing an astrocyte-specific hamster PrP transgene demonstrated an opposite effect, namely neuronal damage in PrP^C-deficient neurons upon prion challenge (Jeffrey *et al*, 2004). The concept of pathogenesis *in trans*, that is, independent of PrP^C expression, is underlined by prior studies and by experiments herein, which demonstrate that the dendrites of CA1 neurons, an early 'clinical target area' in prion infections, are largely devoid of PrP^C (Figure 5D and E). Susceptibility of dendritic structures in this neuroanatomic area has been demonstrated by several techniques in different models of infectious prion disease (Hogan *et al*, 1987; Johnston *et al*, 1997; Brown *et al*, 2001). We note that these structures are strongly labeled by both Sho peptide directed antisera in wt mice (Figure 5A and B), and are distorted and attenuated in prion-infected mice (not shown), as already described by others (Hogan *et al*, 1987; Johnston *et al*, 1997; Brown *et al*, 2001).

Strikingly, Western blot analyses of brains from clinically ill prion-infected mice revealed a dramatic reduction of Sho protein (Figure 7). Because Sho has neuroprotective properties (Figure 6), it seems reasonable to consider whether a loss of Sho may underlie some of the clinical or pathological features of prion disease. In this regard, future studies utilizing *Sprn*$^{0/0}$ mice should prove informative. The mechanism governing the loss of Sho protein during prion infections remains to be determined. While a transcriptional effect seems unlikely (not shown), protein structure may play a role. Since Sho's conserved region coincides with the epicenter of PrP^C misfolding to disease-associated forms such as PrP^{Sc} (Peretz *et al*, 1997, 2001; Beringue *et al*, 2004), conformational alterations in unstructured, cell-anchored Sho (or in Sho shed into the parenchyma, like other GPI-anchored proteins; Parkin *et al*, 2004) may occur upon interaction with PrP^{Sc}. However, this does not explain how altered Sho proteins, should they exist, might be more prone to degradation. Expanding the view to include the concept of aberrant signaling may provide a more useful take on this problem. Assuming that Sho exerts a neuroprotective function, perturbations in this protective pathway could destabilize Sho or lead to a loss of Sho-expressing cells and a commensurate drop in protein level. According to this hypothesis, parenchymal PrP^{Sc} might interfere with the physiological protective activity of Sho *in trans* by virtue of both its aberrant fold and cell biological resemblance to Sho. While new experiments will be required to probe the validity of these concepts and the mechanisms controlling Sho expression, we suggest that Sho is a potential modulator for the biological actions of normal and abnormal PrP.

Materials and methods

Bioinformatics and statistics

Protein alignments were created using the T-COFFEE algorithm and EST searches conducted using UniGene. Data sets for all transfected constructs were assessed for normality ($P>0.10$) by the Kolmogorov–Smirnov test and analyzed by one-way ANOVA, Tukey pairwise comparisons, with significance set at $P<0.05$, using Prism software (v4.0c, GraphPad Inc.).

Mouse lines, husbandry and inoculations

Zrch I Prnp$^{0/0}$ mice and littermates were maintained on a C57/B6 congenic background. Mice for inoculations, either C3H/B6 hybrids (Toronto) or B6 inbred (McLaughlin Research Institute) were inoculated intracerebrally with 30 μl of 0.1% RML-infected brain homogenate diluted in phosphate-buffered saline (PBS) containing BSA (50 mg/ml), penicillin (0.5 U/ml) and streptomycin (0.5 μg/ml). Age-matched non-inoculated or mice inoculated with normal brain comprised negative controls. Clinically ill mice were killed and 10% brain homogenates in PBS were prepared. Proteinase K digestions (50 μg/ml) were performed at 37°C for 1 h. Sho levels were calculated by densitometry (Scion Image) and comparison to a standard curve created from serial dilutions of non-infected brain homogenate. TgCRND8 mice (Chishti *et al*, 2001) on a C3H/C57BL6 outbred background were killed at clinical illness (~8 months) and 10% brain homogenates prepared in 0.32 M sucrose containing protease inhibitors.

Plasmid generation and recombinant protein

The Sho open reading frame was amplified from mouse genomic DNA and inserted between the *Hin*dIII and *Xba*I sites of either pcDNA3 or pBUD.CE4. GFP (Invitrogen). PrP and Sho mutants were generated using methods previously described (Drisaldi *et al*, 2004), with constructs verified by DNA sequencing (details available on

request). cDNA encoding residues 25–122 of the mouse protein was amplified from pcDNA3.Sho and inserted between the *Nde*I and *Bam*HI sites of the pET-19b vector (Novagen) and expressed in *E. coli* BL21(DE3)/RIL (Stratagene). Following induction and lysis, filtered lysate was subjected to Ni^{2+} affinity chromatography (Qiagen), eluted with 250 mM imidazole and dialyzed into 20 mM Tns–Hcl pH8.0, 100 mM NaCl. The polyhistidine tag was removed with enterokinase (Roche). Purity was assessed by SDS–PAGE and concentration estimated using bovine serum albumin standards. Far-UV circular dichroism spectra of recombinant Sho in PBS pH 7.0 and a protein concentration of 0.1 mg/ml were collected at 22°C using a Jasco J-715 spectropolarimeter.

Sho antibody production

The peptide CRRTSGPGELGLEDDE (Sho residues 86–100 plus an N-terminal cysteine) was conjugated to maleimide-activated KLH (Pierce) and injected into New Zealand White rabbits. Alternatively, recombinant Sho was conjugated to KLH using EDC (1-ethyl-3-[3-dimethylaminopropyl] carbodiimide hydrochloride) chemistry (Pierce) and injected into rabbits. Antibodies were precipitated from serum using ammonium sulfate and then affinity purified using the respective peptide (SulfoLink column) or polypeptide (AminoLink Plus Coupling Gel column) immunogens. Epitope positions are shown in Figure 2.

Cell culture and PI-PLC treatment

N2a cells, HEK293 and CGN cells were cultured, transfected and lysed as described previously (Drisaldi *et al*, 2004), except that staining for an activated caspase 3 neo-epitope (Cell Signaling Technology) was used to quantify apoptotic events and conditioned medium from adjacent wells replaced medium on transfected cells. CGN assays represent two or more independent triplicate transfections into *Prnp*$^{0/0}$ cells, with observers being blind to the genotype of transfected test plasmids. For PIPLC treatment, 24 h post-transfection, Sho-transfected N2a cells were washed three times with PBS, and then treated with PI-PLC (Invitrogen) diluted in PBS for 40 min at 4°C. Cells were then washed twice and lysed as above.

Immunocytochemistry and immunohistochemistry

N2a or HEK293 cells 24 h post-transfection were washed with PBS, fixed with 4% paraformaldehyde, washed with PBS, blocked with 2% goat serum, then incubated with either Sho antibody (04SH-1, 6 μg/ml) or PrP antibody (8H4, 1 μg/ml), overnight at 4°C. Following PBS washes, cells were incubated with AlexaFluor488- or AlexaFluor594-conjugated secondary antibodies (Invitrogen; 1:300) for 2 h and then washed three times with PBS. For tissue analysis, mice were saline-perfused. Brains were fixed in Carnoy's fixative (10% glacial acetic acid, 60% methanol, 30% chloroform) bisected and processed. Six-micrometer sections were dried, deparaffinized and taken to TBS (pH 7.2) for incubation with primary antibody at 4°C (anti-Sho 04SH-1 (1:100, this paper), anti-Sho 06SH-3 (1:200, this paper), anti-Sho 06rSH-1 (1:50, this paper), anti-PrP 3F4 (1:20 000; Signet), anti-PrP 7A12 (1:10 000; Li *et al*, 2000), and anti-calbindin D-28K (1:2000; Chemicon). Other antibodies used include anti-Thy-1, R194 (a generous gift from Roger Morris); anti-NSE, rabbit polyclonal from Polysciences Inc.; anti-synaptophysin, SY38 from Chemicon; anti-actin, rabbit polyclonal from Sigma (20–33); and anti-neurofilament H, SMI-32 from Sternberger Monoclonals Inc. For peptide blocking of antibody reactivity, peptide was added in four-fold mass excess to Sho antibody and incubated overnight at 4°C before use. Sections were rinsed in TBS and processed in DakoCytomation EnVision Labelled Polymer, visualized with DAB (3,3′-diaminobenzidine) and counterstained with Harris' hematoxylin. Images were obtained with a Leica DM6000B microscope using a Micropublisher 3.3RTV camera (Q Imaging Inc.) and OpenLab4.0.4 software (Improvision). Images in Figures 5L, M and 6E were de-convoluted using the iterative restoration function in Volocity. For fluorescent double labeling experiments, the secondary antibodies used were AlexaFluor-488 (green) and AlexaFluor-594 (red)-conjugated antibodies (Invitrogen). For immunocytochemistry on CGNs (Figure 6E), cells were fixed 24 h post-transfection in ice-cold methanol for 5 min at −20°C, and then processed and stained.

In situ hybridization

pcDNA3.Sho plasmid was linearized with *Hin*dIII or *Bgl*II to generate antisense and sense probes, respectively, using the DIG RNA labeling kit (Roche). Sections (6 μm) of formalin-fixed brains were cut using an RNase-free blade, mounted and dried overnight at 63°C. Tissue processing and *in situ* hybridization was performed as described by Peterson *et al* (2004). DIG-labeled RNA probes were diluted 1/200–1/400 in hybridization buffer. Alkaline phosphate substrate NBT/BCIP was added, color development performed for 16 h in the dark and slides mounted without counterstaining.

Brain preparation and Western blotting

Mouse whole-brain homogenates were prepared in 0.32 M sucrose containing complete protease inhibitor cocktail (Invitrogen). For preparation of crude membranes, homogenates were spun at 700 *g* for 10 min at 4°C, pellets washed with 1 volume of homogenization buffer, spun again as above, supernatants were pooled then spun at 100 000 *g* for 1 h at 4°C and pellets resuspended in cold 50 mM Tris–HCl, pH 7.4, 150 mM NaCl, 1 mM EDTA, 1% Triton X-100. After spinning (100 000 *g*, 1 h, 4°C) the supernatant was stored at −80°C. Protein was separated on either NuPAGE 4–12% gels (Invitrogen) using the MES buffer system, or by conventional SDS–PAGE using 14% polyacrylamide gels and transferred to either nitrocellulose (PrP blots, 3% BSA block) or PVDF (Sho blots, 5% non-fat skim milk block). Blots were incubated overnight with primary antibodies (D13 or D18 at 0.5 μg/ml for PrP (InPro Inc.), or 04SH-1 or 06rSH-1 Sho polyclonals at 1:500 or 1:2000, respectively, incubated with HRP-conjugated secondary antibody and developed using 'Western Lightning' ECL (Perkin-Elmer). The embryo blot was supplied from Zyagen (San Diego, CA), probed with 04SH-1 and then stripped using 0.2 M glycine pH 2.2, 1% Tween-20, 0.1% SDS, followed by reprobing with D13 antibody

Supplementary data

Supplementary data are available at *The EMBO Journal* Online (http://www.embojournal.org).

Acknowledgements

This work was supported by the Canadian Institutes of Health Research (Grants MOP36377 and MSC46763) and a fellowship to JCW from the Natural Sciences and Engineering Research Council of Canada (PGSD2-319161-2005). We also acknowledge the travel grants from the CIHR-Strategic Training in Health Research (STIHR) initiative and the Canadian Network Centres of Excellence ('PrioNet'). DW is an Alberta Prion Research Institute Scholar. We thank Nathalie Daude and Agnes Lau for bioinformatic analyses, and Janice Robertson, Julie Forman-Kay and Rod Bremner for discussions.

References

Baumann F, Tolnay M, Brabeck C, Pahnke J, Kloz U, Niemann HH, Heikenwalder M, Rulicke T, Burkle A, Aguzzi A (2007) Lethal recessive myelin toxicity of prion protein lacking its central domain. *EMBO J* **26:** 538–547

Behrens A, Genoud N, Naumann H, Rülicke T, Janett F, Heppner FL, Ledermann B, Aguzzi A (2002) Absence of the prion protein homologue Doppel causes male sterility. *EMBO J* **21:** 1–7

Beringue V, Vilette D, Mallinson G, Archer F, Kaisar M, Tayebi M, Jackson GS, Clarke AR, Laude H, Collinge J, Hawke S (2004) PrPSc binding antibodies are potent inhibitors of prion replication in cell lines. *J Biol Chem* **279:** 39671–39676

Bounhar Y, Zhang Y, Goodyer CG, LeBlanc A (2001) Prion protein protects human neurons against Bax-mediated apoptosis. *J Biol Chem* **276:** 39145–39149

Brandner S, Isenmann S, Raeber A, Fischer M, Sailer A, Kobayashi Y, Marino S, Weismann C, Aguzzi A (1996) Normal host prion protein necessary for scrapie-induced neurotoxicity. *Nature* **379:** 339–343

Brown D, Belichenko P, Sales J, Jeffrey M, Fraser JR (2001) Early loss of dendritic spines in murine scrapie revealed by confocal analysis. *Neuroreport* **12:** 179–183

Büeler H, Aguzzi A, Sailer A, Greiner R-A, Autenried P, Aguet M, Weissmann C (1993) Mice devoid of PrP are resistant to scrapie. *Cell* **73:** 1339–1347

Büeler H, Fischer M, Lang Y, Bluethmann H, Lipp HP, DeArmond SJ, Prusiner SB, Aguet M, Weissmann C (1992) Normal development and behaviour of mice lacking the neuronal cell-surface PrP protein. *Nature* **356:** 577–582

Carlson GA, Kingsbury DT, Goodman PA, Coleman S, Marshall ST, DeArmod SJ, Westaway D, Prusiner SB (1986) Linkage of prion protein and scrapie incubation time genes. *Cell* **46:** 503–511

Chen SG, Teplow D, Parchi P, Gambetti P, Autilio-Gambetti L (1995) Truncated forms of the human prion protein in normal brain and in prion diseases. *J Biol Chem* **270:** 19173–19180

Chiarini LB, Freitas AR, Zanata SM, Brentani RR, Martins VR, Linden R (2002) Cellular prion protein transduces neuroprotective signals. *EMBO J* **21:** 3317–3326

Chishti MA, Yang DS, Janus C, Phinney AL, Horne P, Pearson J, Strome R, Zuker N, Loukides J, French J, Turner S, Lozza G, Grilli M, Kunicki S, Morissette C, Paquette J, Gervais F, Bergeron C, Fraser PE, Carlson GA *et al* (2001) Early-onset amyloid deposition and cognitive deficits in transgenic mice expressing a double mutant form of amyloid precursor protein 695. *J Biol Chem* **276:** 21562–21570

Cui T, Holme A, Sassoon J, Brown DR (2003) Analysis of doppel protein toxicity. *Mol Cell Neurosci* **23:** 144–155

Donne D, Viles JH, Groth D, Mehlhorn I, James TL, Cohen FE, Prusiner SB, Wright PE, Dyson HJ (1997) Structure of the recombinant full-length hamster prion protein PrP(29–231): the N terminus is highly flexible. *Proc Natl Acad Sci USA* **94:** 13452–13457

Drisaldi B, Coomaraswamy J, Mastrangelo P, Strome B, Yang J, Watts JC, Chishti MA, Marvi M, Windl O, Ahrens R, Major F, Sy MS, Kretzschmar H, Fraser PE, Mount HT, Westaway D (2004) Genetic mapping of activity determinants within cellular prion proteins: N-terminal modules in PrP^C offset proapoptotic activity of the doppel helix B/B′ region. *J Biol Chem* **279:** 55443–55454

Flechsig E, Manson JC, Barron R, Aguzzi A, Weissmann C (2004) Knockouts, knockins, transgenics and transplants in prion research. In *Prion Biology and Diseases*, Prusiner SB (ed), pp 373–434. Cold Spring Harbor, NY: Cold Spring Harbor Press

Flechsig E, Shmerling D, Hegyi I, Raeber AJ, Fischer M, Cozzio A, von Mering C, Aguzzi A, Weissmann C (2000) Prion protein devoid of the octapeptide repeat region restores susceptibility to scrapie in PrP knockout mice. *Neuron* **27:** 399–408

Hegde RS, Tremblay P, Groth D, DeArmond SJ, Prusiner SB, Lingappa VR (1999) Transmissible and genetic prion diseases share a common pathway of neurodegeneration. *Nature* **402:** 822–826

Hogan RN, Baringer JR, Prusiner SB (1987) Scrapie infection diminishes spines and increases varicosities of dendrites in hamsters: a quantitative Golgi analysis. *J Neuropathol Exp Neurol* **46:** 461–473

Holscher C, Delius H, Burkle A (1998) Overexpression of nonconvertible PrP^C delta114–121 in scrapie-infected mouse neuroblastoma cells leads to trans-dominant inhibition of wild-type PrP(Sc) accumulation. *J Virol* **72:** 1153–1159

Jeffrey M, Goodsir CM, Race RE, Chesebro B (2004) Scrapie-specific neuronal lesions are independent of neuronal PrP expression. *Ann Neurol* **55:** 781–792

Johnston AR, Black C, Fraser J, MacLeod N (1997) Scrapie infection alters the membrane and synaptic properties of mouse hippocampal CA1 pyramidal neurones. *J Physiol* **500** (Part 1)**:** 1–15

Kimberlin RH, Walker CA (1986) Pathogenesis of scrapie (strain 263K) in hamsters infected intracerebrally, intraperitoneally or intraocularly. *J Gen Virol* **67:** 255–263

Kretzschmar HA, Prusiner SB, Stowring LE, DeArmond SJ (1986) Scrapie prion proteins are synthesized in neurons. *Am J Pathol* **122:** 1–5

Kuwahara C, Takeuchi AM, Nishimura T, Haraguchi K, Kubosaki A, Matsumoto Y, Saeki K, Yokoyama T, Itohara S, Onodera T (1999) Prions prevent neuronal cell-line death. *Nature* **400:** 225–226

Lee DC, Sakudo A, Kim CK, Nishimura T, Saeki K, Matsumoto Y, Yokoyama T, Chen SG, Itohara S, Onodera T (2006) Fusion of Doppel to octapeptide repeat and N-terminal half of hydrophobic region of prion protein confers resistance to serum deprivation. *Microbiol Immunol* **50:** 203–209

Li A, Christensen HM, Stewart LR, Roth KA, Chiesa R, Harris DA (2007) Neonatal lethality in transgenic mice expressing prion protein with a deletion of residues 105–125. *EMBO J* **26:** 548–558

Li R, Liu T, Wong BS, Pan T, Morillas M, Swietnicki W, O'Rourke K, Gambetti P, Surewicz WK, Sy MS (2000) Identification of an epitope in the C terminus of normal prion protein whose expression is modulated by binding events in the N terminus. *J Mol Biol* **301:** 567–573

Liu T, Zwingman T, Li R, Pan T, Wong BS, Petersen RB, Gambetti P, Herrup K, Sy MS (2001) Differential expression of cellular prion protein in mouse brain as detected with multiple anti-PrP monoclonal antibodies. *Brain Res* **896:** 118–129

Makrinou E, Collinge J, Antoniou M (2002) Genomic characterization of the human prion protein (PrP) gene locus. *Mamm Genome* **13:** 696–703

McLennan NF, Brennan PM, McNeill A, Davies I, Fotheringham A, Rennison KA, Ritchie D, Brannan F, Head MW, Ironside JW, Williams A, Bell JE (2004) Prion protein accumulation and neuroprotection in hypoxic brain damage. *Am J Pathol* **165:** 227–235

Miesbauer M, Bamme T, Riemer C, Oidtmann B, Winklhofer KF, Baier M, Tatzelt J (2006) Prion protein-related proteins from zebrafish are complex glycosylated and contain a glycosylphosphatidylinositol anchor. *Biochem Biophys Res Commun* **341:** 218–224

Mo H, Moore RC, Cohen FE, Westaway D, Prusiner SB, Wright PE, Dyson HJ (2001) Two different neurodegenerative diseases caused by proteins with similar structures. *Proc Natl Acad Sci USA* **98:** 2352–2357

Moore R, Mastrangelo P, Bouzamondo E, Heinrich C, Legname G, Prusiner SB, Hood L, Westaway D, DeArmond S, Tremblay P (2001) Doppel-induced cerebellar degeneration in transgenic mice. *Proc Natl Acad Sci USA* **98:** 15288–15293

Nishida N, Tremblay P, Sugimoto T, Shigematsu K, Shirabe S, Petromilli C, Pilkuhn S, Nakaoke R, Atarashi R, Houtani T, Torchia M, Sakaguchi S, DeArmond SJ, Prusiner SB, Katamine S (1999) Degeneration of Purkinje cells and demyelination in the spinal cord and peripheral nerves of mice lacking the prion protein gene (*Prnp*) is rescued by introduction of a transgene encoded for mouse *Prnp*. *Lab Invest* **79:** 689–697

Novitskaya V, Bocharova OV, Bronstein I, Baskakov IV (2006) Amyloid fibrils of mammalian prion protein are highly toxic to cultured cells and primary neurons. *J Biol Chem* **281:** 13828–13836

Paisley D, Banks S, Selfridge J, McLennan NF, Ritchie AM, McEwan C, Irvine DS, Saunders PT, Manson JC, Melton DW (2004) Male infertility and DNA damage in Doppel knockout and prion protein/Doppel double-knockout mice. *Am J Pathol* **164:** 2279–2288

Pan KM, Stahl N, Prusiner SB (1992) Purification and properties of the cellular prion protein from Syrian hamster brain. *Protein Sci* **1:** 1343–1352

Parkin ET, Watt NT, Turner AJ, Hooper NM (2004) Dual mechanisms for shedding of the cellular prion protein. *J Biol Chem* **279:** 11170–11178

Peretz D, Williamson RA, Kaneko K, Vergara J, Leclerc E, Schmitt-Ulms G, Mehlhorn IR, Legname G, Wormald MR, Rudd PM, Dwek RA, Burton DR, Prusiner SB (2001) Antibodies inhibit prion propagation and clear cell cultures of prion infectivity. *Nature* **412:** 739–743

Peretz D, Williamson RA, Matsunaga Y, Serban H, Pinilla C, Bastidas RB, Rozenshteyn R, James TL, Houghten RA, Cohen FE, Prusiber SB, Burton DR (1997) A conformational transition at the N terminus of the prion protein features in formation of the scrapie isoform. *J Mol Biol* **273:** 614–622

Peterson KE, Errett JS, Wei T, Dimcheff DE, Ransohoff R, Kuziel WA, Evans L, Chesebro B (2004) MCP-1 and CCR2 contribute to non-lymphocyte-mediated brain disease induced by Fr98 polytropic retrovirus infection in mice: role for astrocytes in retroviral neuropathogenesis. *J Virol* **78:** 6449–6458

Premzl M, Gready JE, Jermiin LS, Simonic T, Marshall Graves JA (2004) Evolution of vertebrate genes related to prion and Shadoo proteins—clues from comparative genomic analysis. *Mol Biol Evol* **21:** 2210–2231

Premzl M, Sangiorgio L, Strumbo B, Marshall Graves JA, Simonic T, Gready JE (2003) Shadoo, a new protein highly conserved from fish to mammals and with similarity to prion protein. *Gene* **314:** 89–102

Prusiner SB, Scott M, Foster D, Pan K-M, Groth D, Mirenda C, Torchia M, Yang S-L, Serban D, Carlson GA, Hoppe PC, Westaway D, DeArmond SJ (1990) Transgenetic studies implicate interactions between homologous PrP isoforms in scrapie prion replication. *Cell* **63:** 673–686

Riek R, Hornemann S, Wider G, Billeter M, Glockshuber R, Wuthrich K (1996) NMR structure of the mouse prion protein domain PrP (121–231). *Nature* **382:** 180–183

Riek R, Hornemann S, Wider G, Glockshuber R, Wuthrich K (1997) NMR characterization of the full-length recombinant murine prion protein, *m*PrP(23–231). *FEBS Lett* **413:** 282–288

Rossi D, Cozzio A, Flechsig E, Klein MA, Rulicke T, Aguzzi A, Weissmann C (2001) Onset of ataxia and Purkinje cell loss in PrP null mice inversely correlated with Dpl level in brain. *EMBO J* **20:** 694–702

Sakudo A, Lee DC, Nakamura I, Taniuchi Y, Saeki K, Matsumoto Y, Itohara S, Ikuta K, Onodera T (2005) Cell-autonomous PrP–Doppel interaction regulates apoptosis in PrP gene-deficient neuronal cells. *Biochem Biophys Res Commun* **333:** 448–454

Scott M, Foster D, Mirenda C, Serban D, Coufal F, Wälchli M, Torchia M, Groth D, Carlson G, DeArmond SJ, Westaway D, Prusiner SB (1989) Transgenic mice expressing hamster prion protein produce species-specific scrapie infectivity and amyloid plaques. *Cell* **59:** 847–857

Shmerling D, Hegyi I, Fischer M, Blattler T, Brandner S, Götz J, Rulicke T, Flechsig E, Cozzio A, von Meering C, Hangartner C, Aguzzi A, Weissmann C (1998) Expression of amino-terminally truncated PrP in the mouse leading to ataxia and specific cerebellar lesions. *Cell* **93:** 203–214

Shyu WC, Lin SZ, Chiang MF, Ding DC, Li KW, Chen SF, Yang HI, Li H (2005) Overexpression of PrP^C by adenovirus-mediated gene targeting reduces ischemic injury in a stroke rat model. *J Neurosci* **25:** 8967–8977

Silverman GL, Qin K, Moore RC, Yang Y, Mastrangelo P, Tremblay P, Prusiner SB, Cohen FE, Westaway D (2000) Doppel is an *N*-glycosylated, glycosylphosphatidylinositol-anchored protein: expression in testis and ectopic production in the brains of Prnp0/0 mice predisposed to Purkinje cell loss. *J Biol Chem* **275:** 26834–26841

Solforosi L, Criado JR, McGavern DB, Wirz S, Sanchez-Alavez M, Sugama S, DeGiorgio LA, Volpe BT, Wiseman E, Abalos G, Masliah E, Gilden D, Oldstone MB, Conti B, Williamson RA (2004) Crosslinking cellular prion protein triggers neuronal apoptosis *in vivo*. *Science* **303:** 1514–1516

Spudich A, Frigg R, Kilic E, Kilic U, Oesch B, Raeber A, Bassetti CL, Hermann DM (2005) Aggravation of ischemic brain injury by prion protein deficiency: role of ERK-1/-2 and STAT-1. *Neurobiol Dis* **20:** 442–449

Sunyach C, Jen A, Deng J, Fitzgerald KT, Frobert Y, Grassi J, McCaffrey MW, Morris R (2003) The mechanism of internalization of glycosylphosphatidylinositol-anchored prion protein. *EMBO J* **22:** 3591–3601

Taraboulos A, Jendroska K, Serban D, Yang S-L, DeArmond SJ, Prusiner SB (1992) Regional mapping of prion proteins in brains. *Proc Natl Acad Sci USA* **89:** 7620–7624

Vincent B, Paitel E, Frobert Y, Lehmann S, Grassi J, Checler F (2000) Phorbol ester-regulated cleavage of normal prion protein in HEK293 human cells and murine neurons. *J Biol Chem* **275:** 35612–35616

Weise J, Crome O, Sandau R, Schulz-Schaeffer W, Bahr M, Zerr I (2004) Upregulation of cellular prion protein (PrP^C) after focal cerebral ischemia and influence of lesion severity. *Neurosci Lett* **372:** 146–150

Wopfner F, Weidenhofer G, Schneider R, von Brunn A, Gilch S, Schwarz TF, Werner T, Schatzl HM (1999) Analysis of 27 mammalian and 9 avian PrPs reveals high conservation of flexible regions of the prion protein. *J Mol Biol* **289:** 1163–1178

